INFLUENCE OF A SCANNING BOX ON THE SETTLING TIME OF MULTI-HOLE PRESSURE PROBES

Johann PUINTNER, Gregor NICHT, Reinhard WILLINGER[1]

[1] Corresponding Author. Institute of Energy Systems and Thermodynamics, TU Wien, Getreidemarkt 9/302, A-1060 Vienna, Austria.
Tel.: +43 1 58801 302403, E-mail: reinhard.willinger@tuwien.ac.at

ABSTRACT

The present paper presents an investigation on the settling time of a measurement setup with following components: multi-hole pressure probe, pressure scanning box, connection tubes, piezoresistive pressure transducer. First, an analytical model is presented to calculate the settling time of such a pressure measurement system. The generic model describes the response time of the pressure transducer due to a sudden jump of the pressure at the probe head. Furthermore, the model is extended to take into account the influence of the scanning box. Second, an experimental campaign is performed to verify the analytical model. For this purpose, a three-hole pressure probe is positioned in the open-jet wind tunnel at constant velocity and yaw angle, to generate large pressure differences between the individual sensing holes. Then, the pressure signals are switched by the scanning box in a sequential manner to the single pressure transducer. The results show that the extended analytical model describes the relaxation behaviour and settling time of the measurement system. The obtained time constant can be used to optimize the experimental process to reduce total measurement time. Finally, some conclusions drawn from the investigation of the sensitivity of the time constant on geometrical parameters are presented.

Keywords: experiment, flow model, multi-hole pressure probe, pressure scanning box, pressure transducer, settling time

NOMENCLATURE

a	[m/s]	speed of sound
c	[m/s]	flow velocity
D	[m]	diameter of replacement tube
d	[m]	diameter of tube
l	[m]	length of tube
m	[kg]	mass
$\dot{m}$	[kg/s]	mass flow rate
n	[-]	total number of tube sections
p	[Pa]	static pressure
Δp	[Pa]	static pressure difference
R	[J/kgK]	specific gas constant
Re	[-]	Reynolds number
T	[K]	temperature
t	[s]	time
t_{99}	[s]	settling time
V	[m³]	volume of plenum
κ	[-]	specific heat ratio
λ	[-]	friction coefficient
ν	[m²/s]	kinematic viscosity
ρ	[kg/m³]	density
τ	[s]	time constant

Subscripts

i	number of tube section
A, B, C	index of volume or pressure at plenum
u	ambient conditions
1, 2, 3	probe hole number

1. INTRODUCTION

Multi-hole pressure probes are frequently used measuring instruments in the experimental field of turbomachinery to determine flow characteristics. Three-hole probes are used for two-dimensional flow fields whereas five-hole probes are able to capture three-dimensional flow fields. By measuring the individual hole pressures, it is possible to derive total pressure, static pressure and flow angles and to draw conclusions about the flow field, including total pressure losses. This is an important advantage of pneumatic measurement methods in relation to optical techniques (LDA, PIV) and hot-wire anemometry (CTA). To obtain a comprehensive overview of the flow, the probe is traversed across a measurement plane, comprising of at least one blade pitch and the blade span, resulting in a large number of measurement points. Figure 1 shows a linear cascade of turbine blades in the wind tunnel of the Institute of Energy Systems

and Thermodynamics. Downstream of the cascade, a three-hole pressure probe is arranged to measure the two-dimensional flow field at midspan. The three individual hole pressures are measured by one single pressure transducer. Therefore, a pressure scanning box is arranged between the three-hole probe and the pressure transducer. The purpose of the scanning box is to switch the pressure signals from the multi-hole pressure probe to one single measurement device. Due to the sequential behaviour of the pressure measurement, the whole process is rather time consuming. Another point to take into account is the individual settling time of the pressure probe, the connection tubes and the pressure transducer.
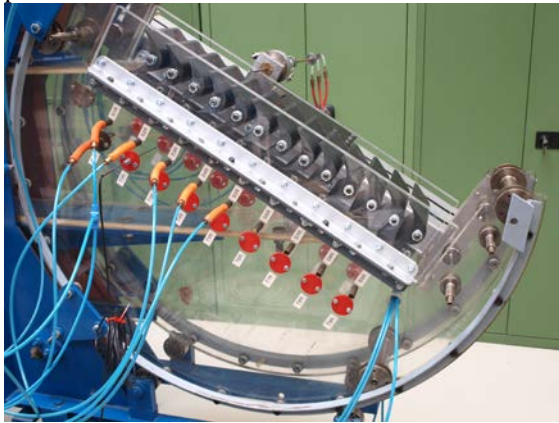

Figure 1. Linear cascade of turbine blades in the wind tunnel

For the planning of the experiment, it is important to know this settling time. On the one hand, the total measurement time should be kept as short as possible. On the other hand, systematic errors will arise, if the waiting time between switching from one pressure channel to the other is too low. This paper presents a combined analytical and experimental investigation on the settling time of multi-hole pressure probes operating with a pressure scanning box.

2. LITERATURE REVIEW

In the open literature, a number of papers can be found which are related to the investigation of the temporal behaviour of pressure measurement systems. From a mathematical point of view, these models can be categorized in first order and second order methods, respectively. If the pressure changes at the probe head appear with high frequency, a second order model is required. This is due to the fact that these models take into account the inertia of the fluid volume in the tubes. As has been pointed out in the introduction, the measurements of interest are steady throughout and a first order model is sufficient. Therefore, the literature review focuses mainly on this kind of models.

An analytical model for the calculation of the response time of gas purged probes connected to a sensitive pressure transducer is presented by Xie and Geldart [1]. The first order model assumes laminar, incompressible flow in the tube and an isothermal change of state in the plenum.

Weidemann [2] gives an analytical and experimental investigation on the inertia of dynamic pressure arrays. The method to calculate a "pneumatic time constant" is based on an electrical analogy.

Sinclar and Robins [3] present an analytical method for the determination of the time lag in pressure measurement systems. The first order model can be categorized into laminar, compressible flow in the tube and an isothermal change of state in the plenum. The main parameters, influencing the response time are analysed. A further objective is to calculate an optimum tube size. Theoretical results are compared with data from systematic experiments.

Lilley and Morton [4] present an analytical method for the calculation of the response time of wind tunnel pressure measurement systems. Additional experiments are performed to validate the analytical model. The detailed model shows that results from simpler methods with concentrated parameters are sufficient to calculate the response time of those systems. However, a prerequisite for sufficient accuracy is to take into account the inlet and exit pressure losses.

A summary of the results from the investigations of [3] and [4] can also be found in the textbook of Wuest [5].

Davis [6] presents a theoretical investigation of the time lag in pressure systems at extremely low pressures. The motivation is that pressure from near vacuum to ambient pressure can appear in transonic and supersonic wind tunnels. Apart from continuous flow, slip flow in the tubes is investigated. This is motivated by the fact that at extremely low pressure, the mean free path is of the same order of magnitude as the diameter of the pressure measuring tube. An experimental check of the validity of the derivation is presented.

Larcombe and Peto [7] provide an analytical method for the calculation of the response time of typical transducer-tube configurations for the measurement of pressure. Since they deal with transonic and supersonic wind tunnels, slip flow as well as continuous flow in the tubes is taken into account. Consideration is given to the special conditions that apply to the case in which the tube systems are connected to a pressure scanning switch.

Bynum et al. [8] provide an overview on wind tunnel pressure measuring techniques. An important aspect is the time response of pressure measuring systems. The report also addresses different options to route tubes from different pressure measurement locations to one single transducer. The authors call this procedure "pneumatic switching". Many

2

practical aspects as well as the influence of the pneumatic switching on the total response time are provided.

Recently, the behaviour of pressure measurement systems working together with multi-hole pressure probes is investigated by Grimshaw and Taylor [9] and Brüggemann et al. [10]. To improve the spatial resolution of the flow measurement in a blade wake, multi-hole pressure probes are more and more miniaturized. On the other hand, this increases the response time of the systems and, therefore, the total measurement time. This trade off is discussed and analysed in the papers. The objective is the accurate prediction of the response time and its minimisation. Both papers use the electrical analogy whereas Brüggemann et al. [10] make also a comparison with results from simpler analytical methods.

3. GENERIC FLOW MODEL

The geometry of the generic flow model, consisting of a tube and a plenum, is shown on top of Fig. 2. The rigid tube with length l has a constant circular cross section with diameter $d \ll l$. The volume of the plenum is denoted as V. The pressure measurement device (transducer) is positioned at the end of the plenum. The bottom of Fig. 2 shows spatial and temporal distribution of static pressure p. At time $t \leq 0$, the constant static pressure in the whole system is p_C (blue line). At time $t = 0$, a sudden jump of the pressure from p_C to p_A is assumed at the inlet of the tube. Due to the pressure difference between the inlet of the tube and the plenum, a flow with velocity c is driven in the tube. Due to the mass flow rate into the plenum, the static pressure in the plenum will increase. After an infinite long time ($t = \infty$), the constant static pressure in the whole system will be p_A.
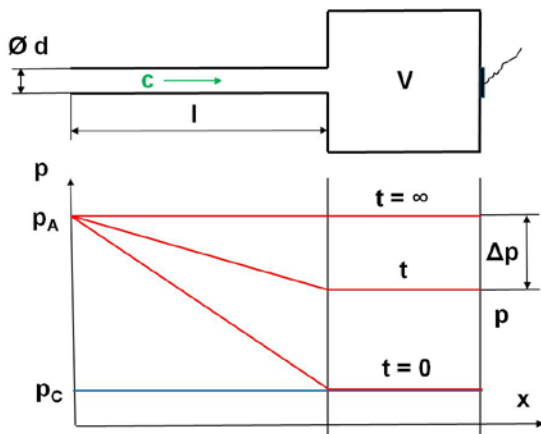

Figure 2. Geometry of generic flow model (top), spatial and temporal pressure distributions (bottom)

Since the pressure difference $p_A - p_C$ is assumed to be small, the density in the tube does not change and the flow can be treated as incompressible. At an arbitrary time t, the pressure loss in the tube is

$$\Delta p = \lambda \frac{l}{d} \rho \frac{c^2}{2}. \tag{1}$$

If the flow is assumed to be laminar, the friction coefficient λ in the tube depends on the Reynolds number according to

$$\lambda = \frac{64}{Re}. \tag{2}$$

As can be seen later, $\lambda l / d \gg 1$. Therefore, the exit loss is neglected in Eq. (1). The mass flow rate driven by the pressure difference Δp is

$$\dot{m} = \rho \frac{d^2 \pi}{4} c = \frac{\pi d^4 \Delta p}{128 l \nu}. \tag{3}$$

A second equation can be derived, if the temporal behaviour of the pressure in the plenum is taken into account. For constant volume V, the change of the fluid mass over time in the plenum is

$$\frac{dm}{dt} = \frac{d(\rho V)}{dt} = \rho \frac{dV}{dt} + V \frac{d\rho}{dt} = V \frac{d\rho}{dt}. \tag{4}$$

If temperature is assumed as constant in the volume, the change of mass over time is

$$\frac{dm}{dt} = \frac{\kappa V}{a^2} \frac{dp}{dt}, \tag{5}$$

with the speed of sound for an ideal gas

$$a = \sqrt{\kappa R T} = \sqrt{\kappa \frac{p}{\rho}}. \tag{6}$$

Since the mass flow rate in the tube (Eq. (3)) is equal to the change of mass over time in the plenum (Eq. (5)), it is

$$\frac{\pi d^4 \Delta p}{128 l \nu} = \frac{\kappa V}{a^2} \frac{dp}{dt}. \tag{7}$$

According to Fig. 2, the pressure loss in the tube is $\Delta p = p_A - p$ and Eq. (7) can be written as

$$\tau \frac{d(\Delta p)}{\Delta p} = -dt, \tag{8}$$

with the time constant

$$\tau = \frac{128}{\pi} \frac{\kappa \nu}{a^2} \frac{l}{d^4} V. \tag{9}$$

3

This time constant can be found in a similar form in [1]. Equation (8) can be integrated for the initial condition $\Delta p(t=0) = p_A - p_C$ and the result is

$$\frac{p - p_C}{p_A - p_C} = 1 - e^{-\frac{t}{\tau}}. \tag{10}$$

The distribution of the nondimensional pressure difference over nondimensional time according to Eq. (10) is plotted in Fig. 3 (red line). The settling time of the system can be defined as the time which is required for the pressure difference to reach 99% of the applied pressure difference ($p_A - p_C$). This nondimensional settling time

$$\frac{t_{99}}{\tau} = 4.6 \tag{11}$$

is indicated by the blue dot in Fig. 3. The green straight line in Fig. 3 gives an interpretation of the time constant τ, since it is the tangent on the red curve at $t/\tau = 0$.
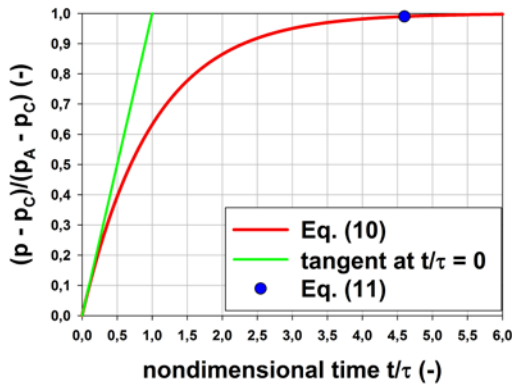

Figure 3. Nondimensional pressure difference versus nondimensional time

According to Fig. 2, the generic flow model is based on one single tube with diameter d and its corresponding length l. In a real measurement setup n tubes with individual diameters d_i and individual lengths l_i are connected in a serial manner. If the first tube with diameter d_1 and length l_1 is defined to set the reference velocity, an equivalent tube length

$$l_e = l_1 + \sum_{i=1}^{n} l_i \left(\frac{d_1}{d_i}\right)^4 \tag{12}$$

can be defined. This equivalent tube length is also introduced in [3]. It can be used for the calculation of the time constant, according to Eq. (9). Another difference between the generic flow model (Fig. 2) and the actual measurement setup is the fact that the pressure scanning box divides the volume V into two separate volumes. These are volume V_A and volume V_B respectively, with

$$V = V_A + V_B. \tag{13}$$

If the valve of the scanning box is closed, both volumes are separated and different pressures will appear in the volumes. Assuming the ideal gas law, it is

$$p_A V_A = m_A R T, \tag{14}$$

$$p_B V_B = m_B R T. \tag{15}$$

A constant temperature T is assumed in both volumes and m_A and m_B are the fluid masses in the individual volumes. If the valve of the scanning box opens very quickly, a mixing process will appear and a pressure p_C will be established in the volume V. If it is assumed that the mixing process is at constant temperature T, the pressure can be calculated according to

$$\frac{p_C - p_B}{p_A - p_B} = \frac{V_A}{V_A + V_B}. \tag{16}$$

4. EXPERIMENTAL APPARATUS AND PROCEDURE

4.1. Open-Jet Wind Tunnel

The open-jet wind tunnel (Fig. 4) consists of a radial blower, a diffuser, a turbulence grid, a settling chamber and a circular cross section nozzle. The radial blower sucks air from the laboratory hall. Therefore, the inlet air temperature is related to the ambient temperature in the laboratory, which is typically about 20 °C. The radial blower is driven by a DC motor with variable rotational speed to set the requested jet velocity at the nozzle. The nozzle with circular cross section (diameter 120 mm) is of Witoszynski type. The contraction ratio between settling chamber and nozzle is about 70:1. The three-hole probe is positioned about one nozzle diameter downstream of the nozzle exit plane. At this section streamwise turbulence intensity in the core of the jet is about 1%.

Figure 4. Open-jet wind tunnel with three-hole pressure probe

4

4.2. Three-Hole Pressure Probe

The present investigation has been performed for a total of five different multi-hole pressure probes. These are three three-hole probes and two five-hole probes, respectively. In this paper, results for one of the three-hole probes are presented. The probe was manufactured in 1994 by SVUSS a.s. [11]. It is a three-hole cobra probe with a characteristic head dimension of 0.8 by 2.4 mm (Fig. 5). The head of the probe consists of three parallel capillary tubes of 0.5 mm inner diameter and 0.8 mm outer diameter, respectively. Hole number "1" is positioned at the centre of the probe head, whereas hole number "2" is on the left hand side and hole number "3" on the right hand side, respectively. A total wedge angle of 60° makes the probe sensitive to variations of the yaw angle in a plane perpendicular to the probe stem. Usually, the probe is operated in the non-nulling mode. The probe stem has a diameter of 6 mm and a total length of 600 mm. Inside of the hollow stem, the capillary tubes of 0.5 mm inner diameter change to capillary tubes of 1.0 mm inner diameter. A stepwise increase of diameters of the capillary tubes inside the probe is a typical provision to reduce their pressure losses. The individual lengths of these capillary tubes are unknown.

Figure 5. Three-hole pressure probe

4.3. Pressure Scanning Box

The pressure scanning box is of type FCO91, manufactured by Furnace Controls Limited [12]. A total of 20 pressure input channels are connected to one single pressure output channel by 20 individual solenoid valves. The solenoid valves can be switched by different operating modes. In the present case, the valves are switched by a current step, produced by the digital output of the data acquisition system. Figure 6 shows a photograph of the scanning box, where the top casing has been dismantled. Inside the casing, the solenoid valves, the internal connection tubes and the electronic equipment can be seen. The internal volumes of the solenoid valves as well as the connection tubes are unknown.
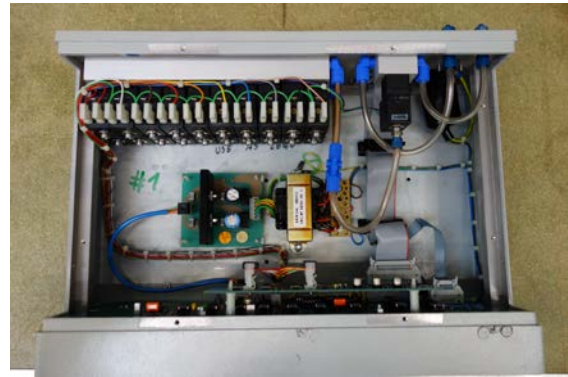

Figure 6. Pressure scanning box (top of the casing dismantled)

4.4. Pressure Transducer

All pressure differences are measured with a HONEYWELL 143PC01D piezoresistive pressure transducer [13]. The operating range of the pressure transducer is ± 69 mbar. One port of the pressure transducer is connected to the output of the pressure scanning box, whereas the other port is open to the atmosphere. Therefore, pressure differences relative to the constant ambient pressure are measured. The pressure transducer is supplied by 8V DC and its output voltage is proportional to the applied pressure difference. A careful inspection of a damaged transducer of the same type has shown that the internal volume of the sensor can be neglected. This means that the transducer does not contribute to the volume V of the plenum.

4.5. Connecting Tubes

Figure 7 shows a schematic representation of the three-hole probe (one capillary tube), the pressure scanning box and the connecting tubes. Inner diameters and tube lengths are summarized in Tab. 1. One single line of the three-hole probe consists of two capillary tubes. Their diameters are 0.5 mm and 1.0 mm, whereas their respective lengths are unknown. The connecting tubes between three-hole probe and pressure scanner, respectively pressure scanner and pressure transducer are of type FESTO. Inner diameter of these plastic tubes is 4.0 mm. The internal volume of the pressure scanning box is approximated by a tube with 4.0 mm inner diameter and length of 0.8 m. On the right hand side, the system is terminated by the pressure transducer. A comparison of the diameters, lengths and volumes of the individual tubes leads to the conclusion that the capillary tubes of the three-hole probe will be responsible for the pressure losses in the system. Therefore, the connecting tubes and the pressure scanning box will contribute to the volume of the plenum. This volume is disconnected by a solenoid valve of the pressure scanning box. To vary the volume of the plenum in a systematic manner, connecting tubes of three different lengths

5

l_5 have been used between scanning box and pressure transducer (Tab. 1).
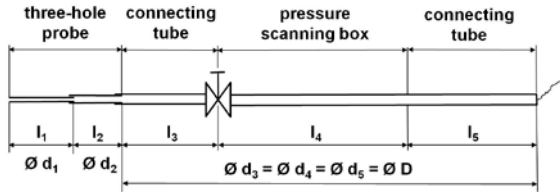

Figure 7. Schematic representation of three-hole probe (one capillary tube), pressure scanning box and connecting tubes

Table 1. Inner diameters and lengths of individual tubes according to Fig. 7

	i	d_i (mm)	l_i (m)
three-hole probe	1	0.5	?
three-hole probe	2	1.0	?
connecting tube	3	4.0	2.0
press. scanning box	4	4.0	0.8
connecting tube	5	4.0	0.5 / 1.0 / 2.0

4.6. Instrumentation

In the settling chamber of the open-jet wind tunnel, total temperature and total pressure are measured my means of a Pt-100 resistor thermometer and wall pressure taps, respectively. The pressure scanning box switches all pressure signals to one single piezoresistive pressure transducer. Control of the scanning box as well as the conversion of the analogue voltages to digital signals is performed by a HP3852A data acquisition system. The system is controlled by a PC, running LabVIEW (National Instruments).

4.7. Measurement Procedure

After the blower of the open-jet wind tunnel has been started, its rotational speed is set to achieve a jet velocity of 48 m/s at the nozzle exit. This corresponds to a probe Reynolds number of about 7500. Then, the three-hole probe is turned by a yaw angle of -30°. At this yaw angle, hole number "2" is at the leeward side and hole number "3" at the windward side, respectively. The objective is to generate large pressure differences between the individual sensing holes. The procedure starts with measurement of total pressure and total temperature in the settling chamber. Then, the pressure signals are switched by the scanning box in a sequential manner to the single pressure transducer, starting with hole number "1". Sampling rate of the data acquisition system is about 6 Hz. Waiting time between switching is set to about 14 seconds. This time is sufficient for the measured pressure difference to reach the final constant value. The measurement procedure is finished when the pressure scanning box is switched from hole number "3" back to the ambient pressure.

5. EXPERIMENTAL RESULTS

5.1. Temporal Pressure Distribution

As a first experimental result, Fig. 8 shows the distribution of the pressure difference, measured by the piezoresistive pressure transducer over time. The results are valid for a tube length $l_5 = 0.5$ m. At the beginning of the procedure ($t = 0$ s), measured pressure difference is zero, since the port of the pressure transducer is connected to the ambient. When the pressure scanning box switches to hole number "1", the pressure difference increases immediately. This pressure jump can be interpreted as the resulting pressure when the mixing process in the plenum is finished. Then, the pressure difference rises rather slowly. This can be interpreted as the pressure rise in the volume due to the mass flow rate through the connected line of the three-hole probe. Finally, a plateau is reached and the pressure difference stays constant. This behaviour is repeated when the scanning box switches from hole number "1" to hole number "2" and from hole number "2" to hole number "3", respectively. The only difference is that holes number "1" and "3" see a positive pressure jump whereas hole number "2" experiences a negative pressure jump. The different final pressure levels of the individual holes are a result of the probe yaw angle. Finally, the measured pressure difference jumps to zero, since the port of the pressure transducer is again connected to the ambient.
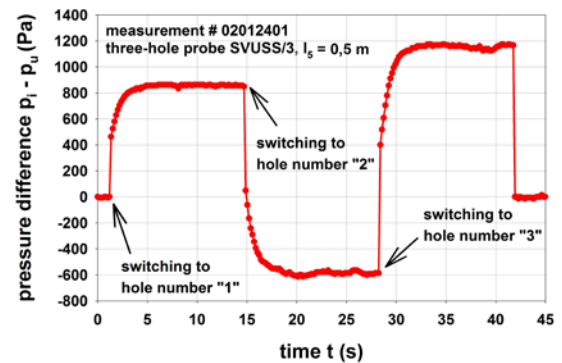

Figure 8. Measured pressure difference ($p_i - p_u$) versus time t ($l_5 = 0.5$ m)

A detailed pressure distribution for the individual holes and three different lube lengths ($l_5 = 0.5$ m, 1.0 m and 2.0 m, respectively) is plotted in Figs. 9 to 11. As can be seen, the tube length l_5 has an influence on the mixing pressure. This can be interpreted by Eq. (16), since the Volume V_B is directly linked to the variable tube length l_5, whereas Volume V_A is constant.
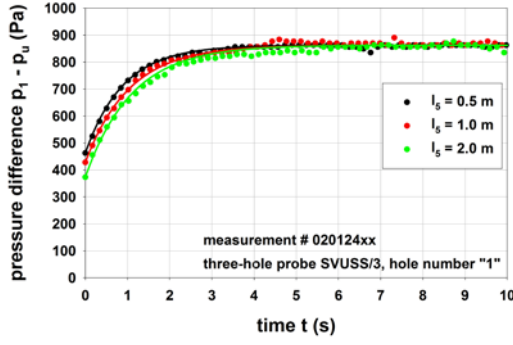
Figure 9. Measured pressure difference ($p_1 - p_u$) for hole number "1" versus time t
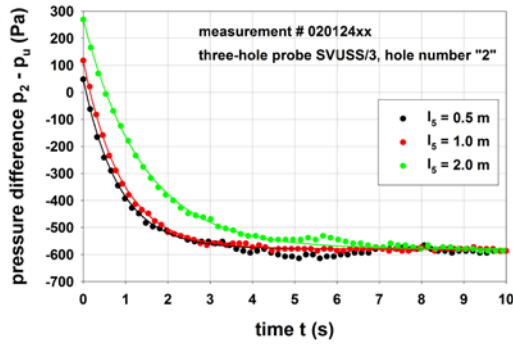

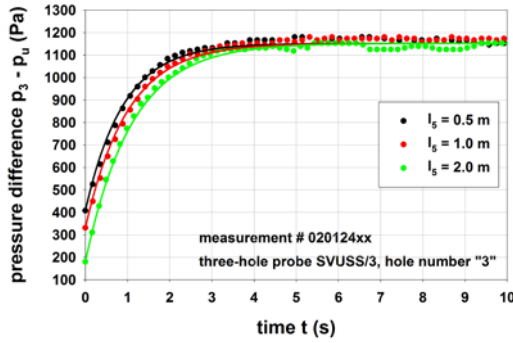**Figure 10. Measured pressure difference ($p_2 - p_u$) for hole number "2" versus time t**

Figure 11. Measured pressure difference ($p_3 - p_u$) for hole number "3" versus time t

Table 2 shows the relative mixing pressure differences $(p_C - p_B)/(p_A - p_B)$ for three different tube lengths l_5. A variation between the individual holes can be seen. Table 2 shows also the arithmetic mean values of the relative mixing pressure differences. As can be seen, the relative mixing pressure differences decrease with increasing tube length l_5. This behaviour can be interpreted using Eq. (16). Since the volumes V_A and V_B are directly related to the tube lengths, it is

$$\frac{p_C - p_B}{p_A - p_B} = \frac{V_A}{V_A + V_B} = \frac{l_3}{l_3 + l_4 + l_5}. \qquad (17)$$

Table 2. Relative mixing pressure difference ($p_C - p_B$)/($p_A - p_B$) from experimental data

	$l_5 = 0.5$ m	$l_5 = 1.0$ m	$l_5 = 2.0$ m
hole "1"	0.536	0.497	0.433
hole "2"	0.564	0.517	0.411
hole "3"	0.570	0.526	0.438
mean value	0.557	0.513	0.427

Results from Eq. (17) are summarized in Tab. 3. For an ideal geometry, there is no influence of individual holes and the relative mixing pressure difference depends on the tube length l_5 only. According to Eq. (17), the relative mixing pressure difference decreases with tube length l_5. A comparison between Tab. 2 and Tab. 3 (grey lines) shows a good agreement between experimental and analytical results. Therefore, the analytical model can be used to describe the mixing process of the pressure measurement setup due to the scanning box.

Table 3. Relative mixing pressure difference ($p_C - p_B$)/($p_A - p_B$) from Eq. (17)

	$l_5 = 0.5$ m	$l_5 = 1.0$ m	$l_5 = 2.0$ m
all holes	0.606	0.526	0.417

5.2. Time Constant and Settling Time

According to the experimental results presented in Figs. 9 to 11, the time constants and the settling time are extracted. In a first step, the temporal behaviour of the pressure difference according to Eq. (10) is fitted to the measurement data. As a result, time constants are extracted for the three different holes related to the tube length l_5. These results are summarized in Tab. 4. As can be seen, there is a variation of the time constants between individual holes. Therefore, arithmetic mean values of the time constant are presented in Tab. 4, too (grey line). As can be seen, time constant increases with increasing tube length l_5. Finally, settling times are calculated according to Eq. (11). For the present measurement setup, settling times are between 4.1 s and 5.5 s, depending on tube length l_5.

Table 4. Time constants τ and settling times t_{99} from experimental data

	$l_5 = 0.5$ m	$l_5 = 1.0$ m	$l_5 = 2.0$ m
τ_1 (s)	0.90	1.05	1.10
τ_2 (s)	0.85	0.90	1.40
τ_3 (s)	0.90	1.00	1.10
τ (s)	0.88	0.98	1.20
t_{99} (s)	4.10	4.50	5.50

According to Eqs. (9) and (12), the time constant of the analytical model is

7

$$\tau = 32 \frac{\kappa \nu}{a^2} \left(\frac{l_1}{d_1^4} + \frac{l_2}{d_2^4} \right) D^2 (l_3 + l_4 + l_5). \qquad (18)$$

A direct application of Eq. (18) to calculate the time constant is not possible, since lengths l_1 and l_2 of the capillary tubes are unknown. However, since it is known that $l_1 + l_2 = 660$ mm, the time constant can be calculated as a function of tube length l_1. The result can be seen in Fig. 12 (lines). For constant tube length l_5, there is a linear relationship between time constant τ and tube length l_1. Also plotted in Fig. 12 are the experimental values for the time constants according to Tab. 4 (dots). A good correlation between analytical and experimental time constants can be obtained for $l_1 \approx 180$ mm. According to the geometry of the three-hole probe, this is a realistic position for the transition of the capillary tubes from $d_1 = 0.5$ mm to $d_2 = 1.0$ mm.
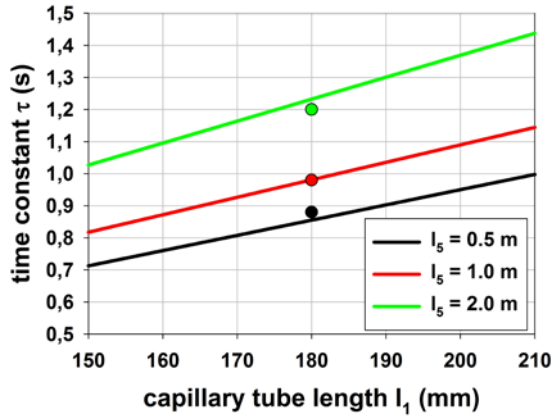

Figure 12. Time constant τ as a function of tube lengths l_1 and l_5

6. FINAL REMARKS

6.1. Reynolds Numbers

The analytical model is based on the assumption that the flow in the capillary tubes is laminar. To justify this assumption, Reynolds numbers which appear in the experiment are calculated. According to Eq. (10), the Reynolds number in the tube with diameter d_1 is

$$Re_1 = \frac{p_A - p_C}{32 \rho \nu^2 \left(\frac{l_1}{d_1^3} + \frac{d_1}{d_2} \frac{l_2}{d_2^3} \right)} e^{-\frac{t}{\tau}}. \qquad (19)$$

This is the larger Reynolds number in both capillary tubes, since

$$Re_2 = Re_1 \frac{d_1}{d_2} < Re_1. \qquad (20)$$

Figure 13 shows the distribution of Reynolds number Re_1 over nondimensional time t/τ for a driving pressure difference $p_A - p_C = 1000$ Pa. This pressure difference is representative for hole number "3" and $l_5 = 2.0$ m (Fig. 11). Reynolds number over time behaves like the mass flow rate or the flow velocity in the capillary tubes. At the beginning of the flow process, Reynolds number shows its maximum value which is still much lower than the critical value $Re_{crit} \approx 2300$. Therefore, the assumption of laminar flow in the analytical model is justified.
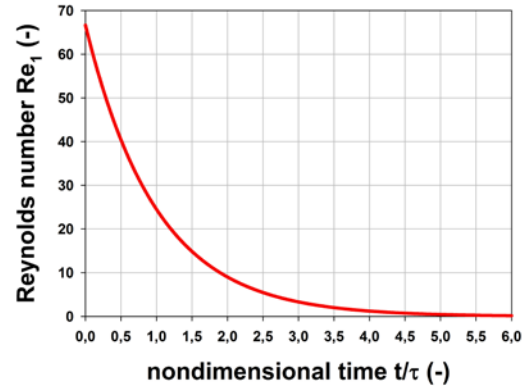

Figure 13. Reynolds number Re_1 versus nondimensional time t/τ

6.2. Uncertainty and Sensitivity

As can be seen from Eqs. (9) or (18), the analytical calculation of the time constant requires the knowledge of the geometry of the pressure measurement system. This means the internal geometry of the multi-hole pressure probe, diameters and lengths of the connecting tubes, the internal volume of the scanning box and, if applicable, the internal volume of the pressure transducer. For a commercial pressure probe, the internal geometry is usually not known. The same is true for a pressure scanning box and a pressure transducer. Therefore, for most practical implementations, it is not possible to calculate the time constant and, therefore, the settling time of the pressure measurement system.

Another aspect is the sensitivity of the time constant on the geometrical parameters of the pressure measurement system. From Eq. (9) it can be derived that the relative sensitivity of the time constant τ to the geometrical parameters l, d and V is

$$\frac{\Delta \tau}{\tau} = \frac{\Delta l}{l} - 4 \frac{\Delta d}{d} + \frac{\Delta V}{V}. \qquad (21)$$

This means that the time constant is very sensitive to the inner diameter d of the capillary tube, which is responsible for the pressure loss. Grimshaw and Taylor [9] state that the inner diameters of tubes for pressure probes (hypodermic

tubes) show typical manufacturing variations of ± 15%. According to Eq. (21), this would result in a variation of the time constant of ± 60%. This high sensitivity can explain the variation of the time constants between different holes of the three-hole pressure probe (Tab. 4). Furthermore, the pressure losses in a multi-hole pressure probe can be influenced by fouling or even clogging due to particles in a non-deterministic manner.

7. SUMMARY

Time constants and settling times for a pressure measurement system, consisting of multi-hole pressure probe, pressure scanning box, connection tubes and a piezoresistive pressure transducer have been investigated experimentally. Detailed results are presented for a configuration with a three-hole cobra probe. The temporal behaviour of the system can be explained by an analytical model. It describes the sudden mixing process of two volumes with different pressure but constant temperature and the response of a tube-plenum system to a sudden pressure jump. Due to the lack of detailed geometrical details of the multi-hole pressure probe and the scanning box, it is usually not possible to calculate time constants and settling times with high accuracy. Therefore, it will still be necessary to determine these parameters for an individual configuration by means of experiments.

REFERENCES

[1] Xie, H.-Y. and Geldart, D., 1997, "The response time of pressure probes", *Powder Technology*, Vol. 90, pp. 149-151.

[2] Weidemann, H., 1941, "Inertia of Dynamic Pressure Arrays", *NACA TM 998*.

[3] Sinclair, A.R. and Robins, A.W., 1952, "A Method for the Determination of Time Lag in Pressure Measuring Systems Incorporating Capillaries", *NACA TN 2793*.

[4] Lilley, G.M. and Morton, D., 1960, "The response time of wind tunnel pressure measuring systems", *The College of Aeronautics Cranfield*, Report No. 141.

[5] Wuest, W., 1969, *Strömungsmesstechnik*, Vieweg & Teubner-Verlag.

[6] Davis, W.T., 1958, "Lag in Pressure Systems at Extremely Low Pressures", *NACA TN 4334*.

[7] Larcombe, M.J. and Peto, J.W., 1966, "The Response Times of Typical Transducer-Tube Configurations for the Measurement of Pressures in High-Speed Wind Tunnels", *Aeronautical Research Council*, C.P. No. 913

[8] Bynum, D.S., Ledford, R.L. and Smotherman W.E., 1970, "Wind Tunnel Pressure Measuring Techniques", *AGARDograph No. 145*.

[9] Grimshaw, S.D. and Taylor, J.V., 2016, "Fast Settling Millimetre-Scale Five-Hole Probes", *ASME Paper GT2016-56628*.

[10] Brüggemann, C., Hobel, S., Schatz, M. and Vogt D.M., 2016, "On the Impact of Tube Dimensions of Pneumatic Probes on the Response Time", *XXII Biannual Symposium on Measuring Techniques in Turbomachinery, Transonic and Supersonic Flow in Cascades and Turbomachines*, September 1 – 2, Stuttgart, Germany.

[11] Konecny, G., 1994, "Eichungsprotokoll der Dreilochsonde 0,8 / 600 – 650", SVUSS a.s., Praha, Czech Republic

[12] N.N., 1995, "Instruction manual FCO91 selection box", Furnace Controls Limited, England.

[13] N.N., 1994/95, "Drucksensoren, Luftstrom-, Temperatur und Füllstandssensoren", Katalog E13, Honeywell.